COSMIC: CARBON MONOXIDE AND SOOT IN MICROGRAVITY INVERSE COMBUSTION

L.G. Blevins[1], M.G. Fernandez[2], G.W. Mulholland[2],
R.W. Davis[3], E.F. Moore[3], E.B. Steel[3], and J.H.J. Scott[3]
[1]Combustion Research Facility, Sandia National Laboratories, Livermore, CA
[2]Building and Fire Research Laboratory, National Institute of Standards and Technology
[3]Chemical Science and Technology Laboratory, National Institute of Standards and Technology

INTRODUCTION

Almost seventy percent of deaths in accidental fires are caused by inhalation of toxins such as carbon monoxide (CO) and smoke (soot) that form during underventilated burning [1,2]. The COSMIC project examines the formation mechanisms of CO and soot during underventilated combustion, achieved presently using laminar, inverse diffusion flames (IDFs) formed between an air jet and surrounding fuel. A major hypothesis of the project is that the IDF mimics underventilated combustion because carbon-containing species that form on the fuel side of the flame (such as CO and soot) can escape without passing through an oxidizing flame tip. An IDF literature review was presented at the last microgravity workshop [3], and a few additional IDF papers have appeared since that meeting [4-6]. The COSMIC project is entering the third year of its four-year funding cycle. The first two years have been devoted to designing and constructing a rig for use in the NASA 2.2-second drop tower. A few computations and laboratory experiments have been performed. The goals of this paper are to discuss the use of numerical simulation during burner design, to present computational and experimental results that support the hypothesis that IDFs are similar to underventilated flames, and to delineate future plans.

COMPUTATIONAL AND EXPERIMENTAL METHODS

Computations of the effects of gravity on methane (CH_4) flame shapes were used to select an appropriate burner design and initial operating condition. Calculations were performed using direct numerical simulation (DNS) of the time-dependent Navier Stokes and conserved variable equations for an axisymmetric laminar flame [7]. The simulation employs assumptions of low Mach number, infinite-rate chemical kinetics (flame sheet), unity Lewis number, variable thermophysical properties, a semi-infinite surrounding fuel-stream, and negligible radiation heat transfer. Dilute-condition particle tracking incorporating the effects of inertial, thermophoretic, and gravitational forces is included [8]. Some particle tracking results are presented here to show basic IDF particle pathways. For the present results, particles are introduced at axial positions of 0 cm, 0.5 cm, 1 cm, 1.5 cm, and 2 cm from the burner and at radial locations corresponding to a characteristic soot formation temperature of 1250 K (see Ref. [9]). Detailed soot modeling is not performed; a recent paper discusses thorough soot modeling for IDFs [4].

For this project, it is desirable to achieve a broad variety of operating conditions that yield different flames in normal-gravity (1-g) and microgravity (0-g) conditions. Initial calculations and experiments were performed using a small (5 mm diameter air jet) co-flow burner chosen for its similarity in size to burners used in previous drop tower experiments [10]. Flame structures were computed for several possible CH_4 operating conditions, and several 1-g flames were stabilized in the laboratory. For all cases in the small burner, the computed IDFs were less than 1 mm long and were unaffected by gravity. In qualitative agreement with this result, laboratory flames were short and steady (similar to micro-flames [11]). Hence, the small burner was found to be undesirable because a wide variety of IDF operating conditions could not be achieved. A larger burner was constructed after identification of desirable dimensions using computations.

The larger burner consists of a 1 cm diameter central air jet surrounded by a 3 cm diameter co-annular fuel tube. A nitrogen (N_2) curtain (6 slpm) flows through a 6.4 cm diameter tube surrounding the burner. The N_2 prevents secondary flames from forming between fuel and room air. Flow-straightening beads and honeycomb are present in the air and fuel passages, while the N_2 flow is smoothed with a fine-mesh screen. The air and fuel tubes are sharpened to knife-like edges to facilitate flame attachment. A propane flare was used downstream of the burner to prevent passage of unburned fuel into the laboratory exhaust duct. For the present paper, one CH_4 flame and one ethylene (C_2H_4) flame were studied. For CH_4, a 46 mg/s (40 sccs or 50 cm/s average velocity) air flow and a 41 mg/s (64 sccs or 10 cm/s) fuel flow were used. For C_2H_4, a 32 mg/s (27 sccs or 35 cm/s) air flow and a 49 mg/s (43 sccs or 7 cm/s) fuel flow were used. The air velocity was five times as large as the fuel velocity for both flames studied. Flame heights were estimated from digital photographs. For the C_2H_4 flame, soot particles were collected on a 3 mm, 400-mesh copper microscope grid coated with amorphous carbon film. The grid was secured to a thin metal spatula and inserted parallel to the flow in the center of the exhaust for five consecutive one-second intervals. The soot particles were analyzed using a Philips CM300FEG Scanning Transmission Electron Microscope (STEM) operating at 300 kV with a 1 nm probe.

RESULTS AND DISCUSSION

Figure 1 depicts temperature contours calculated for the 1-g and 0-g CH_4 flames Representative particle pathways are shown in white. The 0-g flame length (defined by peak temperature) is about 2.2 cm, while the 1-g flame length is 2.1 cm. In agreement with previous findings for laminar jet flames, the computed 0-g flame is longer and more rounded than the 1-g flame [12]. The particle paths shown in Fig. 1 demonstrate that soot particles formed low in the flame move away from the flame for IDFs and can escape with minimal oxidation for both gravity conditions. Figure 2 shows a digital photograph of the 1-g CH_4 flame. The blue flame with orange soot cap is similar to IDFs observed by others [13,14]. The blue portion of the flame is 2.2 cm ± 0.1 cm long, in agreement with the predicted peak-temperature flame height. Despite the existence of the orange soot cap, the soot stream exiting the CH_4 IDF is invisible to the naked eye.

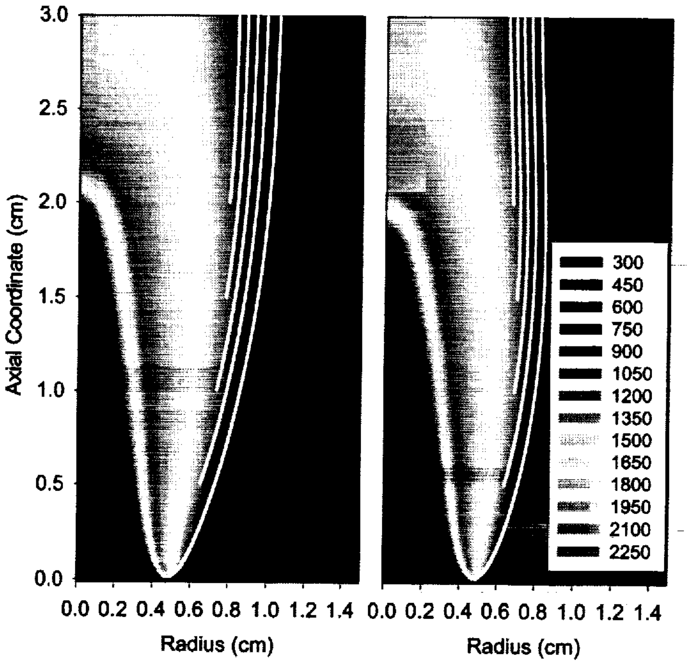

Fig. 1 Calculated absolute temperature (K) for 0-g (left) and 1-g (right) CH_4 IDFs. Half of the axisymmetric domain is shown. White streaks show particle pathways.

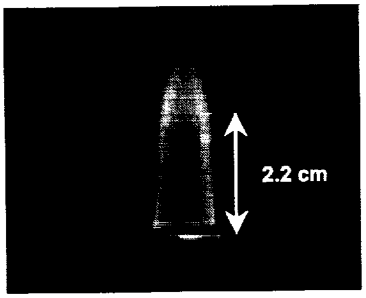

Fig. 2 Photo of 1-g CH_4 IDF.

Figure 3 portrays the calculated time-temperature histories of the particle paths shown in Fig. 1. Particles are tracked until they reach the end of the computational domain (3 cm above the burner). Longer cut-off times for the 0-g particles indicate the lack of buoyant acceleration. In both flames, particles move away from the high temperature region under the influence of thermophoretic forces. Particles in the 1-g flame spend less time at high temperatures than those in the 0-g flame. The implications of this predicted trend for soot structure will be studied in future COSMIC experiments.

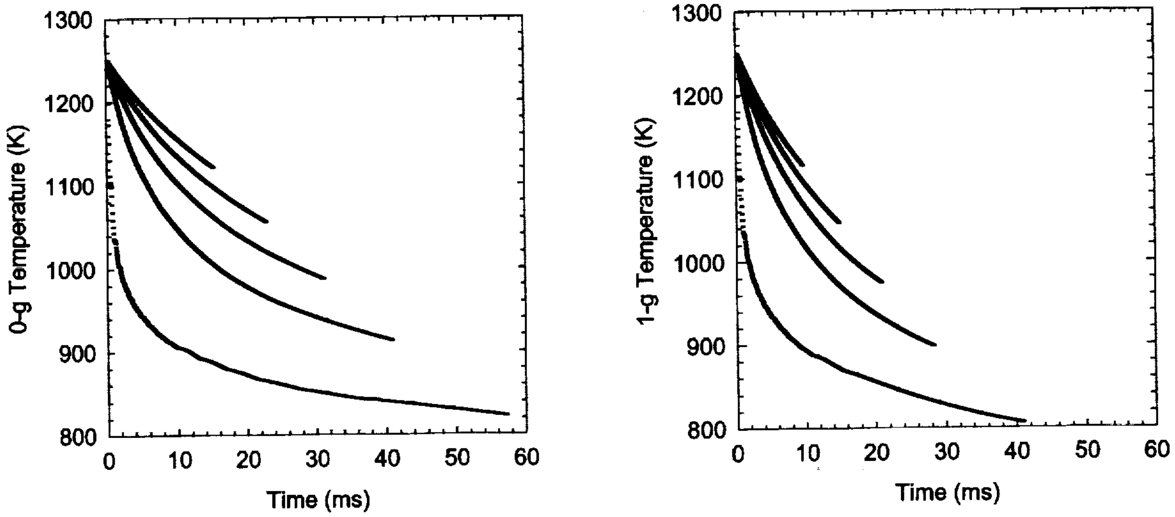

Fig. 3 Time/temperature history of particles in 0-g (left) and 1-g (right) CH_4 IDFs.

A digital photograph of the 1-g C_2H_4 IDF is shown in Fig. 4. The soot cap on the C_2H_4 flame constitutes 90 % of its visible height and its emission intensity saturates the digital camera. The blue portion of the flame is 0.35 cm long, while the total visible flame height is 3.5 cm. A soot stream exits the flame tip (not visible in the dark photograph). The asterisk on Fig. 4 shows the approximate location of soot sampling for the bright-field STEM soot micrograph shown in Fig. 5. The particles appear liquid-like, in agreement with early IDF studies where soot collected on metal targets was sticky and viscous [15-17]. The liquid structure is similar to soot collected in underventilated flame exhaust streams [18] and to soot *precursors* captured from diffusion flames [19]. The major difference between the Fig. 4 soot and that studied in Refs. [18] and [19] is that the present liquid-like structures

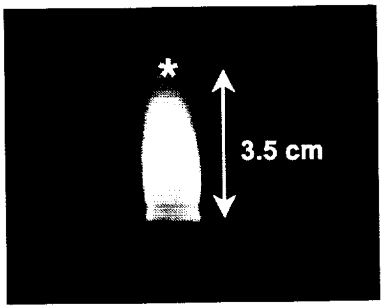

Fig. 4 Photo of 1-g C_2H_4 IDF. An asterisk marks the location of soot sampling.

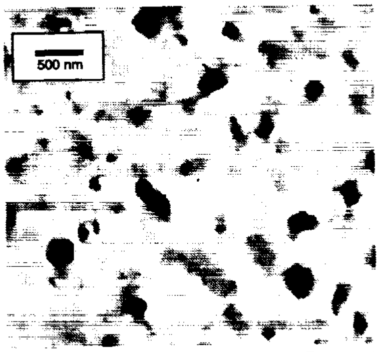

Fig. 5 STEM image of soot collected from 1-g C_2H_4 IDF.

are larger (~250 nm compared to about 20 nm), possibly a result of condensation and coagulation of organic vapors. Particle overlap on the heavily loaded grid could partially explain the large structures, or they may result from post-collection sample transformations. Ongoing efforts are aimed at refining the sampling technique and studying IDF soot structure further.

SUMMARY AND CONTINUING WORK

Direct numerical simulation has been used to guide the design of a burner—relatively large by 2.2-second drop tower standards—and to select initial operating conditions for 0-g and 1-g testing. Two burners were built and tested. Laboratory testing agreed qualitatively with predicted flame height and stability trends. Computed particle pathways revealed that IDF soot is likely to exit flame regions without being fully oxidized. Liquid-like soot samples collected above the flames corroborate this computed result. All of these findings support the major hypothesis that IDF soot (or CO) experiences conditions similar to those encountered by carbon-containing species in underventilated flames. Drop tower experiments employing CH_4 and C_2H_4 IDFs are planned for Summer 2001. Soot yields, CO yields, soot structure, and soot chemical makeup will be studied. The simulation method demonstrated here will be used to predict the paths traveled by soot and CO for the operating conditions studied. Results should provide insight into the formation mechanisms of undesirable CO and soot during underventilated fires.

This research is funded via NASA Contract No. C-32069-J. Dr. Peter Sunderland (technical contact) and Dr. Kurt Sacksteder (technical monitor) provide invaluable assistance.

REFERENCES

[1] Hall, J. R. Jr., Burns, Toxic Gases, and Other Hazards Associated with Fires: Deaths and Injuries in Fire and Non-Fire Situations, National Fire Protection Association (NFPA), Quincy, MA, 1996.

[2] Pitts, W. M., *Progress in Energy and Combustion Science,* 21:197, 1995.

[3] Blevins, L. G., Mulholland, G. W., and Davis, R. W., *Proceedings of the Fifth International Microgravity Combustion Workshop, NASA/CP-1999-208917*, NASA, Cleveland, 1999, p.479.

[4] Kaplan, C. R. and Kailasanath, K., *Combustion and Flame,* 124:275, 2001.

[5] Sung, C. J., Zhu, D. L., and Law, C. K., *Twenty-Seventh Symposium (International) on Combustion,* The Combustion Institute, Pittsburgh, 1998, pp. 2559-2566.

[6] Partridge, W. P., Reisel, J. R., and Laurendeau, N. M., *Combustion and Flame,* 116:282, 1999.

[7] Davis, R. W., Moore, E. F., Chen, L. D., Roquemore, W. M., Vilimpoc, V., and Goss, L. P., *Theoretical and Computational Fluid Dynamics*, 6:113, 1994.

[8] Davis, R. W., Moore, E. F., and Zachariah, M. R., *Journal of Crystal Growth,* 132:513, 1993.

[9] Du, J. and Axelbaum, R. L., *Combustion and Flame,* 100:367, 1995.

[10] Bahadori, M. Y., Edelman, R. B., Stocker, D. P., and Olson, S. L., *AIAA Journal,* 28:236, 1990.

[11] Ban, H., Venkatesh, S., and Saito, K., *Journal of Heat Transfer,* 116:954, 1994.

[12] Sunderland, P. B., Mendelson, B. J., Yuan, Z. G., and Urban, D. L., *Combustion and Flame,* 116:376, 1999.

[13] Sidebotham, G. W. and Glassman, I., *Combustion and Flame,* 90:269, 1992.

[14] Kent, J. H. and Wagner, H. G., *Zeitschrift Fur Physikalische Chemie-Wiesbaden,* 139 :59, 1984.

[15] Arthur, J. R., Commins, B. T., Gilbert, A. S., Lindsey, A. J., and Napier, D. H., *Combustion and Flame,* 2:267, 1958.

[16] Arthur, J. R. and Napier, D. H., *Fifth Symposium (International) on Combustion,* The Combustion Institute, Pittsburgh, 1955, pp. 303-316.

[17] Arthur, J. R., Kapur, P. K., and Napier, D. H., *Nature,* 169:372, 1952.

[18] Leonard, S., Mulholland, G. W., Puri, R., and Santoro, R. J., *Combustion and Flame,* 98:20, 1994.

[19] Dobbins, R. A., Fletcher, R. A., and Chang, H. C., *Combustion and Flame,* 115:285, 1998.